

Analysis for X-Ray Diffraction Pattern of Annealed Fe₂O₃ Thin Films

Mustafa Shakir Hashim, Amira Jawad Kadhim, Reem saadi Khaleel,
Esraa Akram Abbas
Physics department, Education College, Almustansiriya University.

Received Date: 10 / 5 / 2017

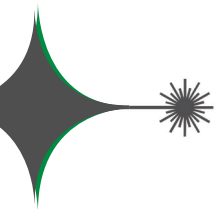
Accepted Date: 16 / 1 / 2018

الخلاصة

وظفت موديلات وليمنسن- هول المعدلة لإيجاد التغيرات في المعلمات التركيبية لأغشية اوكسيد الحديد مع زيادة درجة حرارة التلدين. هذه النماذج هي موديل وليمنسن- هول للمطاوعة الموحدة الخواص، موديل وليمنسن- هول للمطاوعة غير الموحدة الخواص، وموديل وليمنسن- هول لكثافة الطاقة. وحساب الحجم الحبيبي أُستخدِمت معادلة شيرر ومعادلة شير المعدلة، ايضاً حُسِبَ الحجم الحبيبي، مطاوعة الشبيكة، الاجهاد، كثافة طاقة التشوه وكثافة العيوب باستعمال هذه الموديلات. بزيادة درجة التلدين زاد الحجم الحبيبي وفقاً لكل الموديلات. المطاوعة المحسوبة بثلاثة موديلات كانت سالبة وازدادت قيمتها مع زيادة درجة التلدين، وحسب موديل وليمنسن- هول للمطاوعة غير الموحدة الخواص وموديل وليمنسن- هول لكثافة الطاقة فان الاجهاد، كثافة الانخلاعات وكثافة طاقة إجهاد الشبيكة وصلت الى اقل قيمة لها عند درجة (500) مئوي.

الكلمات المفتاحية

هيئة القمة، تلدين، اوكسيد الحديد، معلمات التركيب المايكروي، موديلات وليمنسن- هول.



Abstract

Modified Williamson-Hall (W-H) models were employed to estimate the changing of the microstructural parameters of Fe₂O₃ thin films with increasing annealing temperature (Ta). These models are W-H-anisotropic strain model (W-H-ASM), W-H-isotropic strain model (W-H-ISM) and W-H-energy density model (W-H-EDM). To calculate crystallite size, Scherrer equation and its modified equation were used. Also crystallite size, lattice stress, strain, dislocation density and deformation energy density have been determined by these models. By increasing Ta, crystallite sizes were increased according to all models. Three modified (W-H) models were used to calculate strain, it was negative and its values increase with Ta. According to W-H-ASM and W-H-EDM stress, dislocation density and lattice strain energy density reach minimum values when the temperature reaches (500) °C.

Keywords

Peak Profile, annealing, Fe₂O₃, microstructural parameters, Williamson-Hall models.



1. Introduction

Fe_2O_3 is a metal oxide has many uses [1]. In thin films field, Iron oxide has several applications. Due to its small energy gap and high absorption coefficient it is utilized as solar cell [2]. Fe_2O_3 thin film is being used in flammable gas sensing due to its fast response [3]. This material is easy to fabricate, non toxic, high chemical stability, has environmentally friendly properties, high corrosion resistance and low cost [4]. To expand the applications of Fe_2O_3 thin films its useful to estimate the microstructural properties of these films. X-ray peak profile analysis (XPPA) is important analytical method to verify this estimation. A wealth information like crystallite size, distribution of the phases in the material, strain, stress and other properties are extracted from diffraction lines of crystalline materials [5]. The aim of this contribution is applying W-H models to estimate microstructural parameters of annealed Fe_2O_3 thin films.

1.2. Theory

Bragg peaks are affected by two criteria: changing peak width or shifting peak position. From XPPA there are different models to measure crystallite size, lattice strain, stress and imperfections. The first model is Scherrer model by which crystallite size is calculated using the following equation [6]:

$$\text{Crystallite size} = k\lambda / \beta_{hkl} \cos\theta_{hkl} \quad (1)$$

Where ($k=0.9$) is the shape factor, $\lambda=$

(0.154056) nm is the wavelength of X- rays for radiation of $\text{Cu K}\alpha_1$, in radians β_{hkl} is the widening of the hkl diffraction peak measured at half of its maximum intensity. To estimate more accurately nano-crystallite size; Monshi *et al.* utilized modified Scherrer equation using XRD [7]. The following equation is used to minimize the sources of errors by using the data from all of the available peaks.

$$\ln \beta = \ln k\lambda/L + \ln 1/\cos\theta_{hkl} \quad (2)$$

Where L is crystallite size.

The second model used to calculate lattice strain and crystallite size is (W-H-ISM) model. By assuming that the strain present in milled fishbone is isotropic; the W-H-ISM for complete widening is given by

$$\beta_{hkl} \cos\theta_{hkl} = k\lambda/L + 4\varepsilon \sin\theta_{hkl} \quad (3)$$

Where ε is strain value. If the strain is small and in all crystallographic directions the lattice deformation stress (σ) is uniform, equation (3) can be modified as following

$$\beta_{hkl} \cos\theta_{hkl} = k\lambda/L + 4\sigma \sin\theta_{hkl} / E_{hkl} \quad (4)$$

Where E is Young's modulus. In hexagonal crystals; the crystallographic direction dependent E_{hkl} is given by the next equation [8]:

$$E_{hkl} = ([h^2 + ((h + 2k)^2)/3 + (a_1/c)^2]^2) / (s_{11}(h^2 + ((h+2k)^2)/3)^2 + s_{33}(a_1/c)^4 + (2s_{13}+s_{44})(h^2+(h+2k)^2/3)(a_1/c)^2) \quad (5)$$

Where common elastic compliances for hy-



droxyapatite are $s_{11} = (7.49 \times 10^{-12})$, $s_{13} = (-4 \times 10^{-12})$, $s_{33} = (10.9 \times 10^{-12})$ and $s_{44} = (15.1 \times 10^{-12})$ [9].

If extracted hydroxyapatite is not homogeneous isotropic in nature equation 3 is no longer correct to use. Also if lattice strain energy density (u) is taken into account, proportionality constants of stress-strain relation are no longer independent. By using Hook's law equation 3 will be modified as following

$$\beta_{hkl} \cos \theta_{hkl} = k\lambda/L + 4[\sin \theta_{hkl} (2/E_{hkl})^{1/2}]u^{1/2} \quad (6)$$

Dislocation density (ρ) can be defined as the length of the dislocation lines per unit volume of the crystal [10]. The following equation is used to calculate ρ .

$$\rho = (12^{1/2} \langle \epsilon^2 \rangle^{1/2}) / (d L) \quad (7)$$

Where $\langle \epsilon^2 \rangle^{1/2}$ is root mean squared strain, d interplanar spacing.

2. Experimental part:

On preheated glass substrates, Fe_2O_3 thin films were deposited. The optimum deposition conditions were: the spraying time 5s, temperature of substrate (200) °C, distance between nozzle and substrate was (30±1)cm and filtered air was carrier gas. As a precursor of Fe; the powder of $FeCl_3 \cdot 6H_2O$ (1.6221) g dissolved in (100) ml distilled water. By using magnetic stirrer for (30) minute, complete dissolving of powder inside water was done.

The equation of decomposition is



The thicknesses of films were estimated by weight method, its' average was (450±20) nm. To determine the orientations of Fe_2O_3 miller indices; Shimadzu X-ray diffractometer is used.

3. Results and discussions:

XRD patterns of as deposit and annealed Iron oxide thin films are shown in Fig. (1). In spite of the beginning of formation peaks along (104) and (110) directions, as deposit Fe_2O_3 sample has amorphous structure. After heat treatment, there is a transform to polycrystalline structure with dominant peak (104). Annealed samples have hexagonal phase according to standard card (JCPDS) with number (00033-0664). With increasing of Ta the sharpness of all peaks increases.

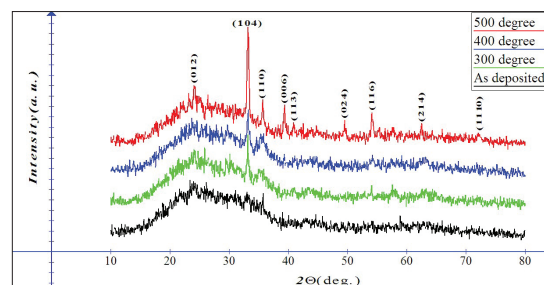


Fig. (1): XRD of as deposit and annealed samples

Equation 2 is used to draw Fig. (2) and then calculate corrected crystallite size.

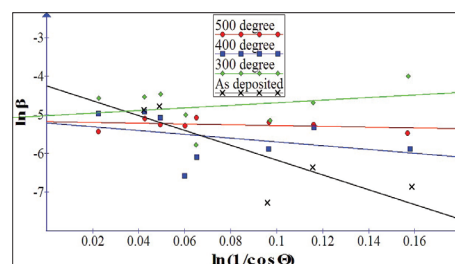


Fig. (2): Application of modified Scherrer equation to find corrected crystallite size.



Fig. (3) illustrates the variation of crystallite size and corrected one as a function to Ta.

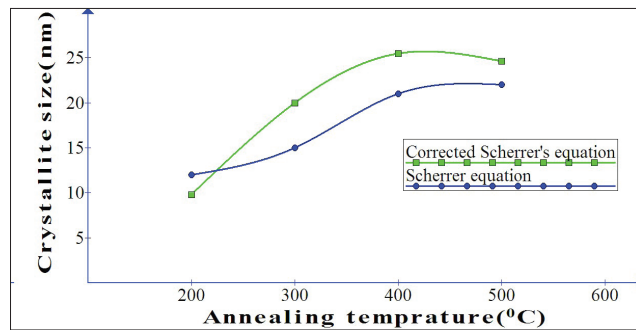


Fig. (3): Annealed crystallite sizes by using Scherrer equation.

Fig. (4) illustrates W-H-ISM plots for as deposited and annealed samples.

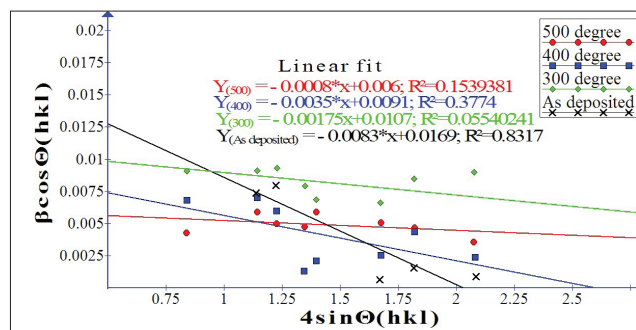


Fig. (4): W-H-ISM plots of annealed samples

Fig. (4) is used to calculate strain and crystallite size according to W-H-ISM model; i.e. using equation 3. The results of this calculation are drawn in Fig. (5). W-H-ISM model is simple technique used to separate between strain induced and size induced peak broadening as Fig. (5) show. Decreasing the total grain boundary energy produces grain growth due to the reductions of free energy [11].

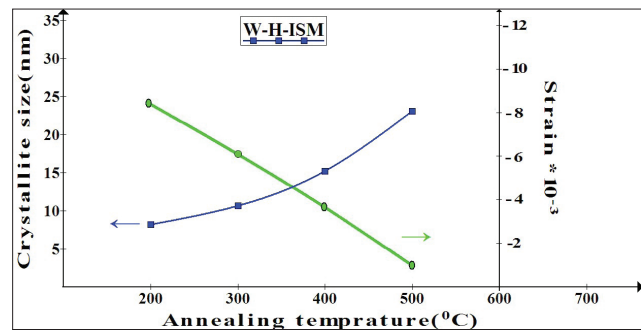


Fig. (5): Determined crystallite sizes and strain (W-H-ISM model).

In the range of current heat treatment the strain decreased with temperature and all strain's values are negative. The lattice strain is negative when crystal lattice is under the influence of compressive forces [12]. The model considers the anisotropic nature of the crystallites is called W-H-anisotropic strain model (W-H-ASM). Fig. (6) Shows $\beta \cos \Theta_{hkl}$ versus $4 \sin \Theta_{hkl} / E_{hkl}$ to calculate stress and crystallite size. Fig.(7) illustrates the effect of Ta on stress and crystallite size.

After calcination; the increase of crystallite size in Fig. (7) can be attributed to the reduction of defects such as dislocations that may appear in different ways [13].

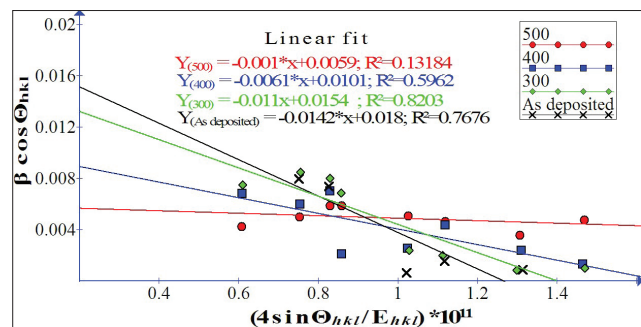


Fig. (6): W-H-ASM plots of annealed samples.

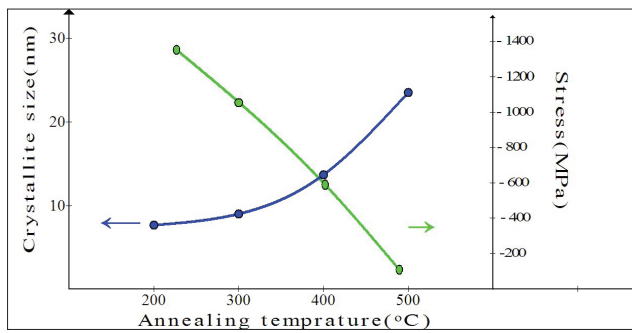


Fig. (7): Calculated crystallite sizes and stress (W-H-ASM model).

The stress reaches minimum value when the temperature reaches (500) °C. The de-

creased stress fields may associate with the reduction of the dislocations that decreased with heat treatment.

Table (1) illustrates calculated strain using the values of stress (calculated from Fig. 6) and $E_{(hkl)}$ (for different Millar indices). The strain values for annealed samples at (500) °C are decreased to approximately one tenth that of as deposited sample. So to remove the stress and strain from milled fishbone heat treatment at (500) °C is appropriate choice.

Table (1): Strain value according to W-H-ASM model.

Millar indices	$E_{(hkl)} * 10^{11}$	$(\epsilon = \sigma / E_{(hkl)}) * 10^{-3}$			
		As deposited	°C 300	°C 400	°C 500
(012)	1.38	-102.899	-79.7101	-44.2	-7.2
(104)	1.38	-102.899	-79.7101	-44.02	-7.2
(110)	1.63	-87.1166	-67.4847	-37.4	-6.13
(006)	0.917	-154.853	-119.956	-66.5	-10.9
(113)	1.63	-87.1166	-67.4847	-37.4	-6.13
(024)	1.63	-87.1166	-67.4847	-37.4	-6.13
(116)	1.63	-87.1166	-67.4847	-37.4	-6.13

W-H-energy density model (W-H-EDM) is used to calculate the strain when the lattice strain energy density u is considered. Fig. (8) shows W-H-EDM plots.

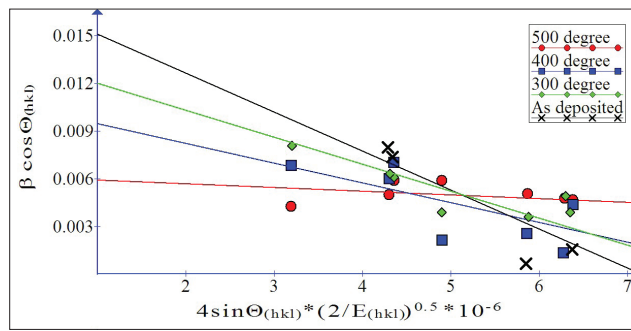


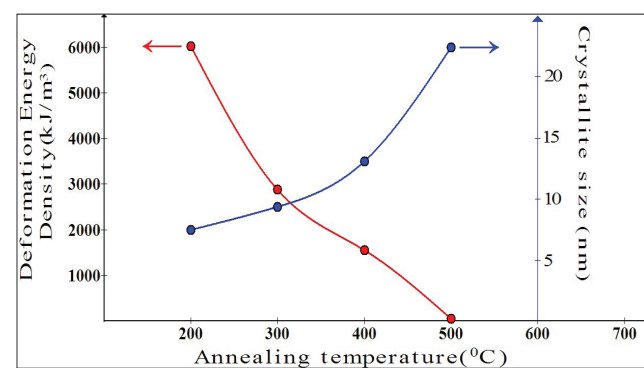
Fig. (8): W-H-EDM plots of annealed samples.

Calculated strain in Table (2) by this model is decreased with temperature but with fewer rates than that obtained by W-H-ASM model. Strain is minimized when smaller structures attach each other to form larger crystallite. It is worth to mention that surface potential is affected by the variation of strain due to its effect on bond lengths and angles [14].

Table (2): Strain value according to W-H-EDM model.

Miller indices	$E_{(hkl)} * 10^{11}$	$\varepsilon = 2u / E_{(hkl)}^{0.5} * 10^{-3}$			
		As deposited	°C (300)	°C (400)	°C (500)
(200)	1.63	-54.87	-45.646	-39.058	-25.901
(002)	0.917	-73.156	-60.857	-52.073	-34.532
(210)	1.59	-55.556	-46.216	-39.546	-26.225
(211)	1.56	-56.09	-46.658	-39.924	-26.476
(300)	1.56	-56.09	-46.658	-39.924	-26.476
(301)	1.51	-57.011	-47.425	-40.580	-26.919
(222)	1.52	-56.82	-47.268	-40.446	-26.822

Fig. (9) illustrates the relationship between deformation energy density and crystallite size as a function to T_a . The heat treatment reduces the lattice strain energy density to its minimum value when the temperature reached (500) °C; this behavior might due to the ability of atoms to take their equilibrium positions at this temperature. We have seen that the crystallite sizes still increase with T_a , this confirms the improving of crystallinity of films with annealing.

Fig. (9): Deformation energy density and crystallite size versus T_a .



The dislocation density is defined as the length of dislocation lines per unit volume. From the theoretical point view a dislocation within the crystal is a defect or a crystallographic irregularity. The defects inside the crystal have direct effect on the characteristic of the formed crystal [16].

.Fig. (10) shows the relationship between dislocation density and Ta

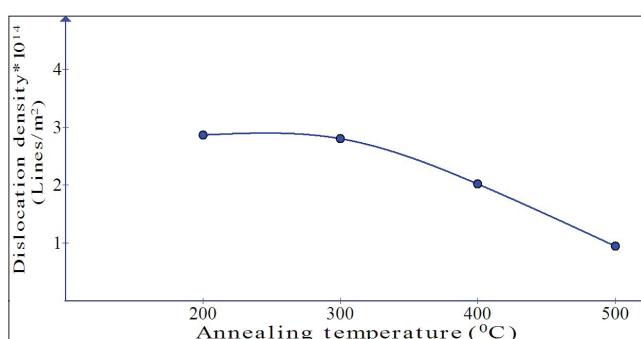


Fig. (10): Dislocation density versus Ta.

Dislocation density decreases to low value as Ta increases. So crystals with smaller dislocation density were less hardness. The formation of multiple linear defects specially dislocations which produce high dislocation density regions in the grains piling up irregular clusters into grains [15].

After X-ray diffraction line profile analysis of nano BaSr₆Fe₄TiO₃ prepared by solid state method; Reenu Jacob and Jayakumari Isac confirmed that crystals of this material with larger dislocation density were harder. Also they found that the dislocation density increases while crystallite size decreases with increasing strain [16]. In current work; increasing of Ta produces larger crystallite size and smaller dislocation density.

The fundamental Bragg reflection can be effected by point defects (their effect on peak profile is called Huang scattering) and by dislocations. The first factor has short- range field order and the second has long- range order field [17]. The effect may appear as a shift in peak shifts (like planar defect) or peak broadening and peak shifts simultaneously (like stacking faults). Dislocation always present as a major component of lattice defects or as the only lattice defect present inside crystal lattice [14]

4. Conclusions:

- 1- In a reasonable approximation; the W-H models can be used to calculate microstructural parameters such as lattice deformation stress , lattice strain, and lattice deformation energy density.
- 2- To remove the stress and strain from Fe₂O₃ thin films heat treatment at (500) °C is appropriate choice.
- 3- Dislocation density decreases to low value as Ta increases.
- 4- The structure of Fe₂O₃ can change from amorphous to crystalline by increasing oxidation level during annealing process.
- 5- The present analysis can be used for understanding the stress and the strain present in the thin films through annealing.
- 6- The three modified forms of W-H analysis were helpful to define the crystal perfection,



References:

- [1] P., Mallick, and B. N. Dash. Nanoscience and nanotechnology. 3(5),130-134, (2013).
- [2] J.H.Kennedy, and D.J.Dunnwald. Electrochem. Soc. 130 , 2013-2016,(1983).
- [3] K.Siroky, Jana Jirešová and Lubomír Hudec. Thin Solid Films. 245(1-2), 211-214, (1994).
- [4] T.Hahn, Nathan, Heechang Ye, David W Flaherty, Allen J Bard and C Buddie Mullins. Acs Nano. 4 (4),1977-1986, (2010) .
- [5] E.J. Mittemeijerv, and U. Welzel. Z.Kristallogr. 223, 552–560, (2008).
- [6] S. Vives , E. Gaffet, C. Meunier. Materials Science and Engineering. A366,229-238,(2004).
- [7] A. Monshi , M. Reza Foroughi , M. Reza Monshi. World Journal of Nano Science and Engineering. 2, 154-160,(2012).
- [8] Y. Taraka Prabhu , K. Venkateswara Rao, V. Sesha Sai Kumar , B. Siva Kumari. World Journal of Nano Science and Engineering. 4, 21-28, (2014).
- [9] D. E. Gray, American institute of physics handbook, New York McGraw-Hill Book company,(1972).
- [10] B.E.Warren, E.P. Warekois. Acta Metallurgica 3, 473-479,(1955).
- [11] H. Zhang, B. Chen, and J.F. Banfield. Phys Chem. Chem. Phys. 11, 2553–2558, (2009).
- [12] H. Zhang and J.F. Banfield. J. Phys. Chem. B 104, 3481–3487, (2000).
- [13] S. Miraghaei, P. Abachi, HR. Madaah-Hosseini, A. Bahrami. J Mater Process Technol.203(1-3), 554-60, (2008).
- [14] T. Ungar , J. Gubicza , G. Ribarik , C. Pantea, T. Waldek Zerda. Carbon 40, 929–937, (2002).
- [15] S.Sivasankaran,K. Sivaprasad,R.Narayanasamy and P.V. Satyanarayana. X-ray peak broadening analysis of AA 6061100 – x –x wt.% Al₂O₃ nanocomposite prepared by mechanical alloying. Materials characterization 62 (2 0 1 1) 6 6 1 – 6 7 2.
- [16] R. Jacob and J. Isac. International Journal of Chemical Studies. 2(5),12-21, (2015).
- [17] H.Trinkaus, Phys Stat Sol (b). 51, 307–19,(1972).

